Placenta 82 (2019) 46–56

Contents lists available at ScienceDirect

Placenta

journal homepage: www.elsevier.com/locate/placenta

Placentation in the Blue Wildebeest (*Connochaetes taurinus*)

Sandra Wilsher*,[1], Fiona Stansfield, WR(Twink) Allen[1]

The Paul Mellon Laboratory of Equine Reproduction, "Brunswick", 18 Woodditton Road, Newmarket, Suffolk, CB8 9BJ, UK

ARTICLE INFO

Keywords:
Wildebeest
Placenta
Cotyledon
Caruncle
Placentome
Binucleate cell

ABSTRACT

Introduction: The wildebeest is a populous African ungulate, but despite its wide distribution within that continent few reports exist on the structure and endocrine functions of its placenta.

Methods: The pregnant uteri of 43 Blue Wildebeest estimated to be at less than 70 days of the 8 month gestation period were examined grossly and histologically.

Results and discussion: The cervix divided into left and right components which eliminated any connection between the uterine horns and limited conceptus development and placentation to the single ipsilateral horn. The placenta was typically ruminant synepitheliochorial macrocotyledonary with numerous flat placentomes developing in the gravid horn. Appreciable quantities of exocrine secretion were accumulated in the lumen of both gravid and non-gravid uterine horns and proliferation of the trophoblast into presumptive villi was evident between the placentomes. The single corpus luteum of pregnancy persisted unchanged during the period of gestation monitored and the mononuclear trophoblast cells of the intercotyledonary, but not the cotyledonary, allantochorion stained strongly for 3-β hydroxysteroid dehydrogenase indicating their likely secretion of progesterone. The binucleate trophoblast cells stained positively with antisera raised against placenta-associated glycoprotein and bovine placental lactogen. Neither the maternal corpus luteum or the allantochorion showed immunohistochemical staining for cytochrome P450 aromatase.

1. Introduction

The wildebeest (*Connochaetes sp.*) is a populous, middle-sized, grazing ruminant that is distributed widely throughout the savannahs and grasslands of central, eastern and southern Africa. Very large populations (i.e. > 1,000,000) migrate annually through the Serengeti-Masai Mara ecosystem on the borders of southern Kenya and northern Tanzania where they show a remarkably synchronised mating which results in about 80% of the population calving in a 3-week period to minimise predation of the newborn calves by large felids and hyena [1,2]. Elsewhere they show a less restricted breeding season which commences in late April/early May at the end of the long rains [3]. In both migratory and resident wildebeest populations it is estimated that > 90% of adult females conceive during each season [1].

Female wildebeest are seasonally polyoestrous and spontaneously ovulate a single follicle during an oestrous cycle of around 23 days which includes a 14–15 day luteal period [1,4]. The cervix is Y-shaped, dividing into left and right cervical canals about two-thirds of the way along its length. Each of these then merges into the left or right uterine horns respectively, thereby ablating the existence of a conventional intercommunicating uterine body (Fig. 1a and b) [5,6], making the uterus essentially duplex, like that of the gemsbok (*Oryx gazelle gazelle*), roan (*Hippotragus equinus*), addax (*Addax nasomaculatus*) and sable antelopes (*H. niger*) [5]. Gestation in the wildebeest has been estimated from mating and calving peaks to range from 8 to 9 months [1,3]. However, in a more recent study when mating and calving were observed in identified animals, the gestation length was closer to 8 than 9 months with a mean ± SEM of 241 ± 11.7 days followed by a post-partum anoestrus of 104 ± 16 days [4]. The single conceptus always implants in the uterine horn ipsilateral to the side of ovulation [1] and it develops a typical ruminant macrocotyledonary placenta which, due to the aforementioned duplex uterus without connection between the horns, remains confined to that ipsilateral horn. This means it attaches to and interdigitates with only around half of the 70 (58–104) cotyledons arranged in four rows throughout the two uterine horns [7–9]. Birth occurs very rapidly and the precocious newborn calf usually stands within 6 min, suckles and can gallop alongside its mother shortly thereafter, albeit slightly unsteadily for the first hour *post partum* [2,3].

Hradecký et al. [8] gave a brief description of the microscopic structure of the placentome of a wildebeest with a 45 cm crown-rump length (CRL). The villi were described as being branched throughout the entire thickness of the placentome, with irregular shapes in cross-

* Corresponding author.
E-mail address: sandrawilsher@hotmail.co.uk (S. Wilsher).
[1] Present address; The Reproduction Laboratory, Sharjah Equine Hospital, P.O. Box 29858, Sharjah, UAE.

https://doi.org/10.1016/j.placenta.2019.05.008
Received 16 March 2019; Received in revised form 14 May 2019; Accepted 17 May 2019

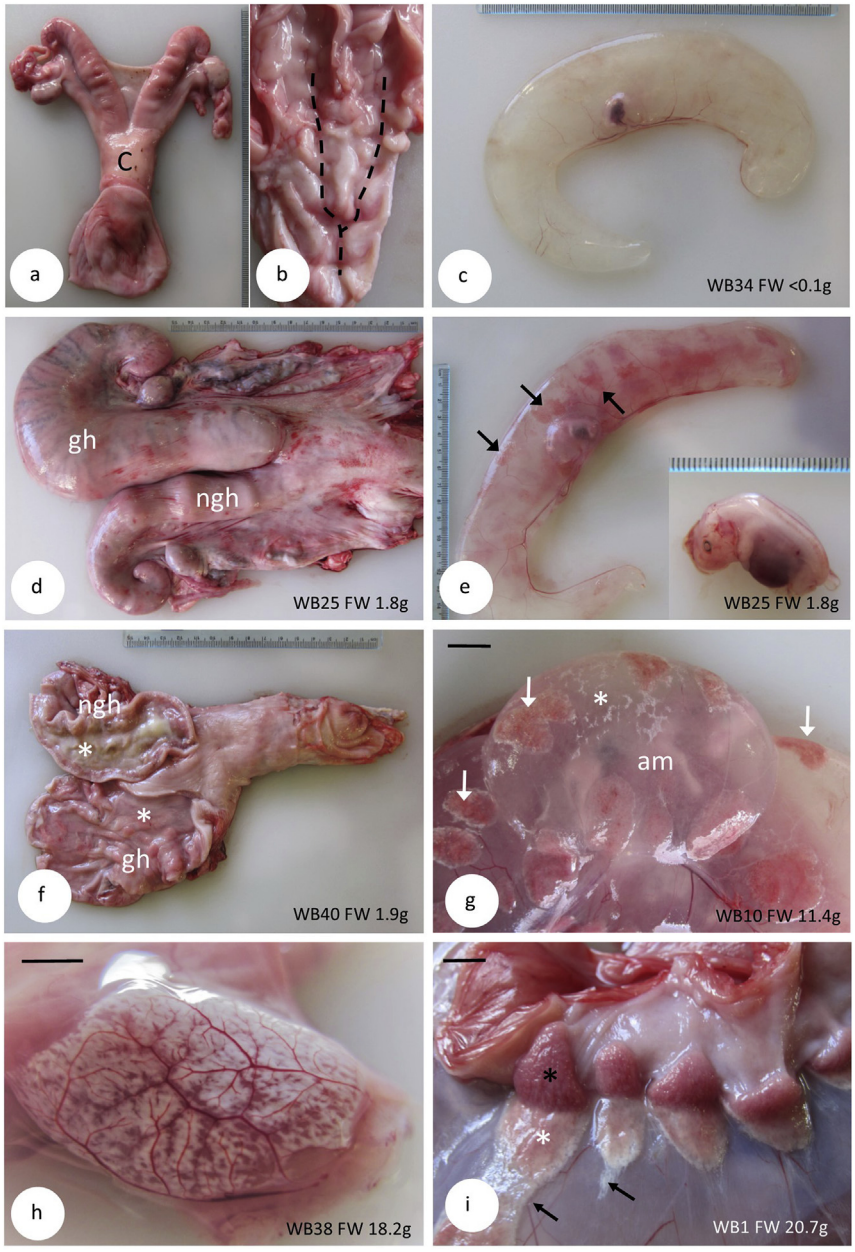

Fig. 1. a) Non-gravid reproductive tract of a young, prepubertal wildebeest (WB). Note the lack of uterine body and the large, thickened cervix (C).
b) Cervix opened to show how it divides before entering each uterine horn (dotted line).
c) Intact conceptus from WB34 (fetal weight [FW] < 0.1 g). The embryo is encased in its amnion and the main artery and vein supplying the allantochorion have developed along the lesser curvature of the conceptus.
d) The intact pregnant uterus and ovaries from WB25 (FW = 1.8 g). Note the clear difference between the gravid horn (gh) and non-gravid horn (ngh).
e) The intact conceptus from (d) and its 1.8 g fetus (inset). Note the cotyledons just starting to develop on the surface of the allantochorion (arrowed).
f) The opened uterus from WB40 (FW = 1.9 g). The conceptus has been removed to show the accumulation of endometrial secretions or histotroph (asterisk) accumulated in both the gravid horn (gh) and non-gravid horn (ngh). Note the inspissated nature of the secretions in the non-gravid horn.
g) The conceptus from WB10 (FW = 11.4 g). The fetus is enclosed in its amnion (am) overlain by the allantochorion and the developing fetal cotyledons can be seen on the allantochorion (arrowed). The asterisk highlights the areas of intercotyledonary trophoblast growth (scale bar = 2 cm).
h) A placentome from WB38 (FW = 18.2 g) viewed through the still attached allantochorion to show the complex distribution of chorionic blood vessels over its surface (scale bar = 0.5 cm).
i) Placentomes in the uterus of WB1 (FW = 20.7 g) being pulled apart to illustrate their fetal cotyledon (white asterisk) and maternal caruncle (black asterisk) components. The black arrows indicate the tendency for the fetal cotyledons to over-run their area of attachment to the maternal caruncles (scale bar = 1 cm).

section and moderate surface corrugation. The mesenchymal cores of the villi were noted to be thin with only a few blood vessels and the lining of the crypts was syncytial in nature. More recently, it has been shown that the wildebeest is the first bovid to show a continuous syncytial fetomaternal layer like that of the sheep and goat, rather than the small infrequent syncytial patches that occur in the cow and deer [10].

There is also limited information on the endocrinology of pregnancy in the wildebeest. Clay et al. [4] collected faecal samples from wildebeest and determined that fecal progestagen concentrations during pregnancy were around twice those attained during the luteal phase of the oestrous cycle. But apart from this, nothing has been recorded to date about embryonic, fetal and placental development in the wildebeest, nor have the endocrinological capabilities of the wildebeest placenta been examined. This paper addresses these aspects following a rare opportunity to examine grossly, histologically and immunocytochemically the gravid uteri of 43 adult Blue Wildebeest culled for management reasons during the first third of their gestation.

2. Materials and methods

2.1. Tissues

The uteri and ovaries from a total of 43 pregnant wildebeest were brought to a dissection table within 3 h of death where they were photographed intact before the ovaries were removed, bisected, photographed and weighed. Each uterus was opened along its gravid and non-gravid horns to expose the intact conceptus within its allantochorion still attached to the endometrial caruncles in the ventral portion of the gravid horn. The allantochorion was opened and samples of the allantoic and amniotic fluids were recovered and frozen, together with the serum decanted from a post mortem jugular vein blood sample collected prior to butchering the carcass. Small whole placentomes, or pieces of larger placentomes, were dissected and fixed in 10% neutral buffered formaldehyde solution (NBF).

The embryo/fetus was removed and weighed for subsequent calculation of the stage of gestation using the formula created by Widdas and Huggett [11]. Fetal gender was noted and crown-rump length

Table 1
Primary antibodies used in the study.

Antibody specificity	Trade name	Source	Dilution	Manufacturer
3β hydroxysteroid dehydrogenase (3βHSD)	3β HSD (37-2): (sc-100466)	Mouse monoclonal raised against recombinant 3β-HSD of human origin	1: 100	Santa Cruz Biotechnology, Inc., Santa Cruz, CA, USA
Cytochrome P450 aromatase	MCA2077S	Mouse monoclonal raised against a synthetic peptide corresponding to amino acids 376 – 390 of human aromatase.	1: 5000	AbD Serotec, Raleigh, NC, USA
Bovine placental lactogen	bPL	Rabbit polyclonal raised against bovine placental lactogen	1: 1000	Gifted by: Dr Peter Wooding, The Physiology Laboratory, University of Cambridge, UK
Placenta-associated glycoprotein (PAG)	PAG-RB (MF = RB)	Rabbit polyclonal raised against bovine PAGs	1:1000	Ditto

(contour from poll to base of tail) measurements were taken.

2.2. Histology and immunocytochemistry

Pieces of the NBF-fixed placentomes, intercotyledonary allantochorion, maternal endometrium and ovary recovered from each animal were trimmed, dehydrated through a graded series of alcohol concentrations, embedded in paraffin wax and sectioned at 5 μm. One section from every block was mounted on normal microscope slides and stained with haematoxylin and eosin (H&E) for conventional histology, and additional sections from every block were layered onto positively charged slides for immunocytochemical staining in a Dako Autostainer as described previously [12].

Details of the four primary antibodies used in this study are given in Table 1. Negative controls were run by replacing each primary antibody with an unrelated rabbit or mouse-generated antibody. In addition, reproductive tissues from other species known to stain negatively or positively with the antibody in question were used as controls.

2.3. Hormone assays

The peripheral sera and the allantoic and amniotic fluid samples collected were assayed for progestagen concentration using an amplified enzyme-linked immunoassay (AELIA) [13]. The limit of detection of the assay was 0.135 ng/ml and the intra- and interassay coefficients of variation were 6 and 8%, respectively. The antiprogesterone monoclonal antibody used in the assay was reported to exhibit cross-reactivities of 100% with progesterone, 56% with 11α-hydroxyprogesterone 19% with 5α-pregnane-3,20-dione, 17% with aetiocholon-3α-ol-17-one and 3% with 17α-hydroxyprogesterone. Dilution curves generated by a pool of pregnant wildebeest serum with a high concentration of progesterone and male wildebeest serum spiked with progesterone were parallel to the curve produced by the equine progesterone standards.

3. Results

The weight, gender and other parameters of the embryos/fetuses recovered from the pregnant uteri are listed in Table 2. The pregnancies were all calculated to be ≤ 67 days of gestation.

3.1. Gross anatomy

Placentation: In the 8 youngest specimens (fetal weight < 2.0 g) the conceptus had the form of an elongated, fluid-filled, crescent-shaped sac (Fig. 1c) lying apparently unattached or weakly attached to the endometrium along almost the entire length of the gravid uterine horn; the tip of the horn remained unoccupied in two of the specimens. Even at these early stages the gravid horn was easily distinguishable from the non-gravid horn (Fig. 1d). One of these early pregnant uteri was resorbing the conceptus as indicated by a degenerating embryo and a bloodless allantochorion. The primitive embryo, with its prominent cardiac chamber occupying the space between its vestigial fore and hind limb buds, lay enclosed within the amnion roughly at the centre of the elongated tube-like conceptus (Fig. 1e). Even in the specimens with embryos of < 0.1 g, presumptive cotyledons could be seen on the chorionic surface of the allantochorion (Fig. 1c) and in the slightly later stage specimens (< 2.0 g) red, slightly roughened patches on the surface of the chorion (Fig. 1e) indicated early cotyledon development. Each patch was vascularised by branches from the principal allantoic vessels which ran along the lesser curvature of the tubular conceptus (Fig. 1e). Perhaps most striking, even at this early stage of gestation, were copious amounts of exocrine secretion in both the gravid and non-gravid uterine horns; this accumulated material was remarkably viscous and purulent in appearance in the non-gravid horn (Fig. 1f).

As placental development progressed the oval or circular vascular areas on the chorionic surface of the allantochorion representing the presumptive fetal cotyledons became more prominent, as did the caruncles in the endometrium (Fig. 1g–i). The cotyledons, which showed a flat profile, were arranged in rows on the surface of the allantochorion, corresponding to the underlying caruncles (Fig. 1i; 2a & b). The placentomes situated towards the tip of the horn were less advanced in development than those in the middle and caudal sectors (Fig. 2a). With advancing gestation the surface of each cotyledon became increasingly roughened due to development of the chorionic villi (Fig. 2b), while the caruncles, from which they were easily detached, became increasingly pitted and stippled to accommodate the chorionic villi (Fig. 2c). Endometrial histotrophic secretion was still accumulated around the edges of the caruncles (Fig. 2c).

In the later stage specimens, endometrial secretion was less obvious in the gravid horn, although it was still accumulated in large amounts in the non-gravid horn (Fig. 2d). Irregular, slightly raised white patches of trophoblast tissue could be seen scattered in the intercotyledonary areas of the allantochorion (Fig. 1g; 2a, b & e). These were more prominent in the later stage specimens and, in some instances, seemed to be arranged in irregular rows running between adjacent cotyledons (Fig. 2a and b). Examination of intercaruncular endometrium showed the maternal epithelium to be cellular with no evidence of migration or fusion of the BNCs from the fetal tissue, although it was difficult to collect maternal tissue that was known to have been in direct contact with the intercotyledonary patches of trophoblast tissue as these were not adhered to the underlying maternal tissue at dissection.

In the most advanced specimens, the gravid uterine horn was now much larger and more prominent than the non-gravid horn (Fig. 2f). No fusion of the allantochorion to the amnion was evident and in all specimens the amniotic sac enclosed the fetus but did not extend further along the gravid horn (Fig. 2e). No allantoic calculi or hippomanes were present within the allantoic cavity.

Maternal ovaries: In all 43 pregnant wildebeest the ovary ipsilateral to the conceptus contained a single, large, red-to-red-brown corpus luteum (CL) of pregnancy (Fig. 2g and h). Based on the weights of the ovaries, the CL did not increase or decrease in size as pregnancy

Table 2
Reproductive parameters of 43 pregnant wildebeest.

Animal ID no.	Lactating	Progestagens (ng/ml)			Ipsilateral ovarian weight (g)	Contralateral ovarian weight (g)	Gravid horn	Fetal weight (g)	Gestational age (days)[a]	Fetal gender	Crown-rump length (cm)[†]
		Maternal serum	Allantoic fluid	Amniotic fluid							
WB15‡	No	3.5	–	–	3.3	2.3	L	< 0.1	< 45	–	–
WB27	No	3	–	–	2.2	1.8	R	< 0.1	< 45	–	–
WB34	No	3.2	–	–	2.0	1.1§	L	< 0.1	< 45	–	–
WB46	Yes	2	–	–	2.9	2.2	L	0.7	< 45	–	–
WB3	No	5.6	–	–	2.3	2.4	R	1.4	< 45	–	–
WB11	No	3.5	8	1.5	4.1	2.0	R	1.6	< 45	–	3.0
WB25	No	3.3	11.7	1.2	3.1	2.7	L	1.7	< 45	–	–
WB40	No	2.7	–	–	3.3	1.6	R	1.9	48	–	4.4
WB16	No	4.5	15.7	0.6	2.1	1.5	L	5.1	51	F	4.8
WB28	Yes	4	–	–	3.7	2.2	L	6.1	52	M	6.4
WB53	No	2.4	–	–	3.1	2.7	R	6.3	53	F	5.8
WB35	Yes	2.8	–	–	3.0	2.5	R	6.4	53	M	–
WB18	No	2.2	6.5	1.5	3.0	2.1	R	7.9	54	M	6.7
WB14	No	2.9	16.6	1.6	3.0	2.4	L	10.9	56	F	7.8
WB12	No	4.2	19.5	–	3.4	2.3§	R	11.1	56	F	8.2
WB10	No	4.9	15.5	–	2.2	1.6	L	11.4	56	F	7.6
WB37	Yes	2.1	7.9	0.5	2.7	1.3	L	11.5	56	M	8.1
WB50	Yes	2.6	–	–	2.5	1.5	L	13.2	57	M	8.4
WB36	No	2.3	1.3	1.4	2.1	1.1	R	13.8	57	F	8.1
WB42	No	2	–	–	2.1	1.3	R	13.9	57	M	8.2
WB17	No	28	6.9	1.1	2.8	2.2	R	14.0	57	M	8.3
WB21	No	2	13.5	1.6	5.4	3.4§	L	15.1	58	F	7.8
WB45	Yes	3.6	–	–	2.8	1.8§	L	17.8	59	M	8.4
WB38	No	1.6	15.5	1.8	3.3	1.1§	R	18.2	59	M	8.9
WB33	No	2.1	10.7	0.9	2.7	1.1	L	19.0	59	F	8.7
WB41	No	1.5	–	–	2.0	2.0	R	20.3	60	F	9.4
WB1	No	–	–	–	2.2	1.2	L	20.7	60	F	9.6
WB24	No	2	18.6	–	2.1	1.4	L	21.1	60	M	9.2
WB39	No	2.4	19.1	2.1	2.1	2.1	L	21.8	60	F	8.8
WB4	No	–	–	–	3.4	2.7	R	22.6	60	M	9.1
WB2	No	–	20.3	–	2.8	2.1	R	23.3	61	M	9.0
WB47	Yes	3.2	–	–	2.4	1.6	L	26.0	61	F	10.2
WB48	No	2.2	–	–	3.0	1.5	L	26.2	62	F	10.0
WB9	No	5.1	–	–	3.6	1.8	L	26.2	62	F	–
WB15a	No	3.4	–	–	2.5	1.5	L	27.0	62	M	10.4
WB55	No	2.5	–	–	2.5	1.5	L	29.6	63	M	10.2
WB6	No	–	–	–	2.9	1.8	R	31.1	63	M	11.0
WB44	No	3.2	–	–	3.6	1.8	L	34.6	64	M	10.4
WB49	No	2.8	–	–	2.7	1.6	L	35.0	64	F	11.2
WB20	No	4.7	14.4	4.4	2.7	1.6	R	35.8	64	M	11.0
WB31	No	4.1	26.8	7.4	2.8	1.5	L	39.7	65	M	10.4
WB32	No	2.2	8.8	7.7	2.4	1.2	R	46.0	66	M	12.4
WB13	No	4.4	16.5	6.2	3.0	1.7	R	47.3	67	F	–

[a] Estimated using the formula of Huggett and Widdas [11] as used by Watson [1]; †crown rump was calculated from the poll to the tip of the tail; ‡the pregnancy in this animal appeared to be resorbing; § tissue with the appearance of regressing *corpora albicans* could be seen on this ovary.

advanced (Table 2). Macroscopically, collections of small follicles (2–5 mm diameter) were scattered throughout the stroma of the ovary contralateral to the side of ovulation (Fig. 2g) and, subjectively, appeared to lessen as pregnancy progressed. In 5 of the wildebeest ovaries examined the contralateral ovary also contained tissue with the appearance of a *corpora albicans* (Fig. 2g), sometimes overlain by a fading ovulation stigmata on the surface of the ovary. The wildebeest in which these were seen are noted in Table 2.

3.2. Histology and immunocytochemistry

Histologically, initial development of the placentome was revealed as a series of shallow indentations in the lumenal surface of the caruncle (Fig. 3a and b) in which small clumps of columnar trophoblast cells from the cotyledons on the surface of the allantochorion, especially large binucleate cells (BNCs), remained attached to the flattened epithelial cells of the endometrium (Fig. 3b). An extensive capillary network was forming in the underlying endometrial stroma which included densely packed fibroblasts interspersed with larger maternal blood vessels. Loose accumulations of small, dark staining cells, thought likely to be lymphocytes, were accumulated at intervals within the less dense, capillary-filled, endometrial stroma (Fig. 3b). Although the delay between death and collection and fixation of the placental tissues had caused separation of the allantochorion and endometrium in young placentomes, the continuing adherence of small patches of trophoblast cells to the lumenal epithelium indicated the likelihood of some degree of physical fusion between maternal and fetal tissue (Fig. 3b).

With advancing gestation the continuing upward expansion of the capillary-rich stromal tissue of the endometrial caruncle, and the increasing penetration of this stroma by branching villi of allantochorion, caused the resulting placentome to enlarge. At the stages of pregnancy examined in the present study the placentomes were flat rather than convex or concave (Fig. 3c). The stroma immediately beneath the placentome was especially dense and, beneath this layer, the endometrial glands were distended to varying degrees by accumulated secretion (Fig. 3c), presumably the source of the copious amounts of endometrial secretion present within the lumina of both gravid and non-gravid uterine horns (Fig. 1f). The intercotyledonary allantochorion was closely apposed, but not physically attached, to the endometrium and consisted of both uninucleate cells (UNCs) and BNCs (Fig. 3d).

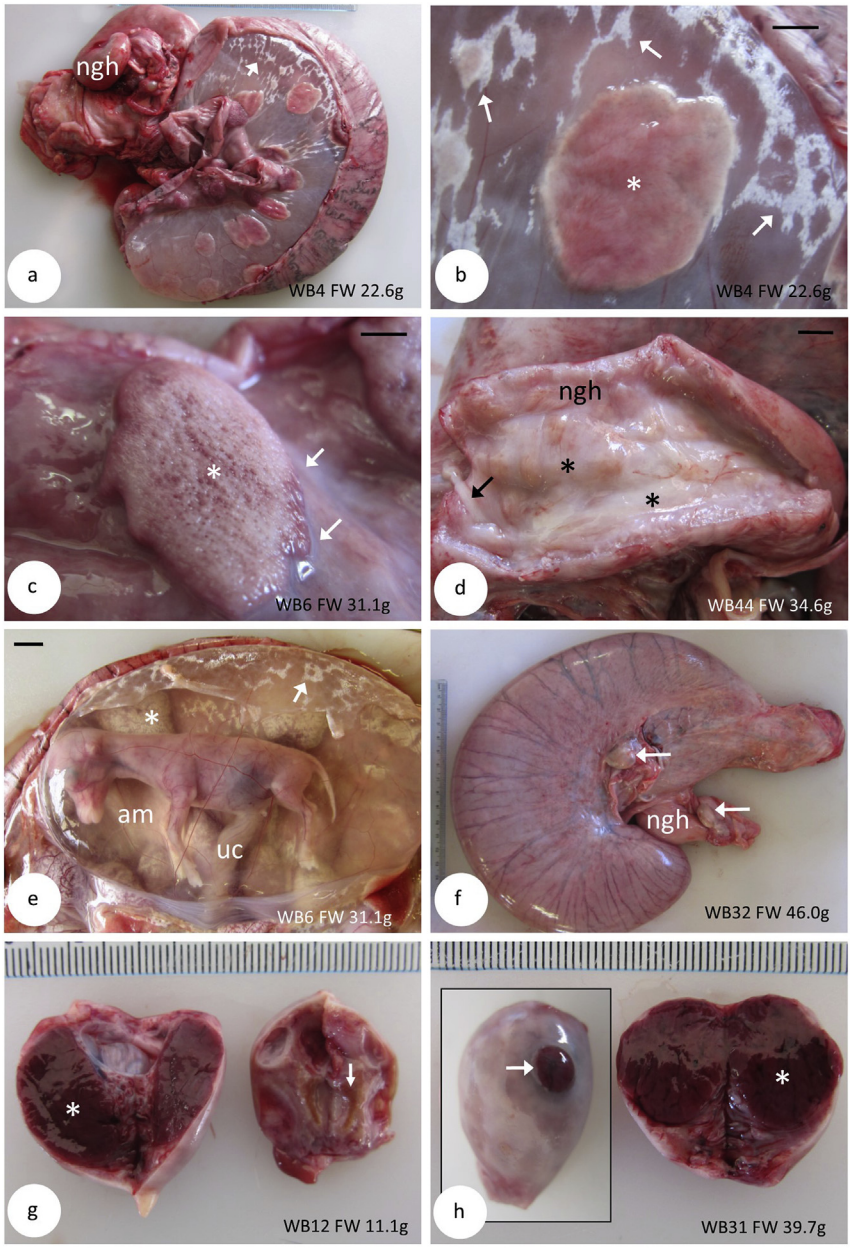

Fig. 2. a) Opened uterus of WB4 (FW = 22.6 g) showing the intact conceptus in the gravid horn. Parallel lines of cotyledons are seen on the allantochorion with small areas of trophoblast growth between the cotyledons (arrowed; ngh = non-gravid horn).
b) Close-up view of a cotyledon (asterisk) and the associated areas of intercotyedonary trophoblast growth (arrows) on the allantochorion of WB4 (scale bar = 0.5 cm).
c) The surface of a maternal caruncle after removal of the cotyledon in WB6 (FW = 31.1 g) showing the pitted surface (asterisk) into which the interdigitating villi of the cotyledon fitted. Maternal histotroph has accumulated around the base of the caruncle (arrowed; scale bar = 0.5 cm).
d) Interior of the non-gravid uterine horn (ngh) in WB44 (FW = 34.6 g). Accumulated histotroph (asterisks) is present in the lumen of the uterine horn and can be seen exuding from the open end (arrow; scale bar = 1 cm).
e) The surface allantochorion removed from WB6 (FW = 31.1 g) to expose the fetus *in situ* in its amnion (am). The umbilical cord (uc) can be clearly seen. Placentomes are visible underneath the amnion (asterisk) and intercotyledonary trophoblast is present on the allantochorion overlying the periphery of the amnion (arrowed; scale bar = 1 cm).
f) Intact unopened uterus of WB32 (FW = 46.6 g) showing the marked expansion of the gravid horn compared to the non-gravid horn (ngh). The ovaries are arrowed.
g) Bisected ovaries from WB12 (FW = 11.1 g). The CL of pregnancy (asterisk) occupies almost all of the right ovary and the remnants of a *corpus albicans* is present in the left ovary (arrowed).
h) Ovary from a WB31 (FW = 39.7 g) sectioned to show the single large CL (asterisk) of pregnancy. The inset shows the ovulation stigma (arrow) on the external surface of the ovary before it was sectioned.

As gestation advanced the placentome became increasingly complex with further branching and interdigitation between the downgrowths of trophoblast villi and corresponding upgrowths of maternal caruncular tissue (Fig. 3e–f). At higher magnification areas where the BNCs were fusing with maternal epithelial cells could be observed (Fig. 3g). The roughened intercotyledonary patches scattered on the allantochorion proved to be undulations of the trophoblast layer (Fig. 3h).

Immunohistochemical labelling of the maternal CL with the 3β hydroxysteroid dehydrogenase (3βHSD) antiserum showed positive staining in both the small and large luteal cells throughout the period of pregnancy studied (Fig. 4a–c). Staining was granular in the large cells (Fig. 4b) and, subjectively, more intense than in the small luteal cells (Fig. 4a–c).

From early in gestation the intercotyledonary trophoblast showed positive, but patchy, staining for 3βHSD which was confined to the UNCs (Fig. 4d and e). In contrast, the trophoblast in the placentomes did not stain at all, whereas the antibody did strongly highlight a subpopulation of red blood cells in both the maternal and fetal capillaries (Fig. 4f and g). This pattern of staining persisted unchanged during the period of pregnancy studied (Figs h & i).

Neither the CL, nor the placentome (Fig. 5a) or intercotyledonary allantochorion, stained with cytochrome P450 aromatase (aromatase). Conversely, the same three tissues stained positively for bovine placental lactogen (bPL) and staining was evenly distributed across all the luteal cells at all stages of gestation studied (Fig. 5b). In the placentomes, staining was confined to the BNCs and the apposing maternal epithelial cells at the base of the placentome (Fig. 5c). The BNCs, but not the UNCs, in the intercotyledonary allantochorion stained with the bPL antibody; this was particularly evident in the areas where the trophoblast had formed the previously mentioned roughened patches (Fig. 5d and e). Subjectively, with advancing pregnancy the maternal stroma in the placentome showed pale staining with the bPL antibody, very likely as a result of transfer of the placental lactogen from the fetal binucleate cells to the maternal tissues (Fig. 5f).

An antibody specific for Pregnancy Associated Glycoprotein-RB (PAG-RB) stained fetal and maternal cells within the placentome from the earliest stages of gestation (Fig. 6a). Staining was particularly intense in the BNCs (Fig. 6b) and was widely dispersed throughout the

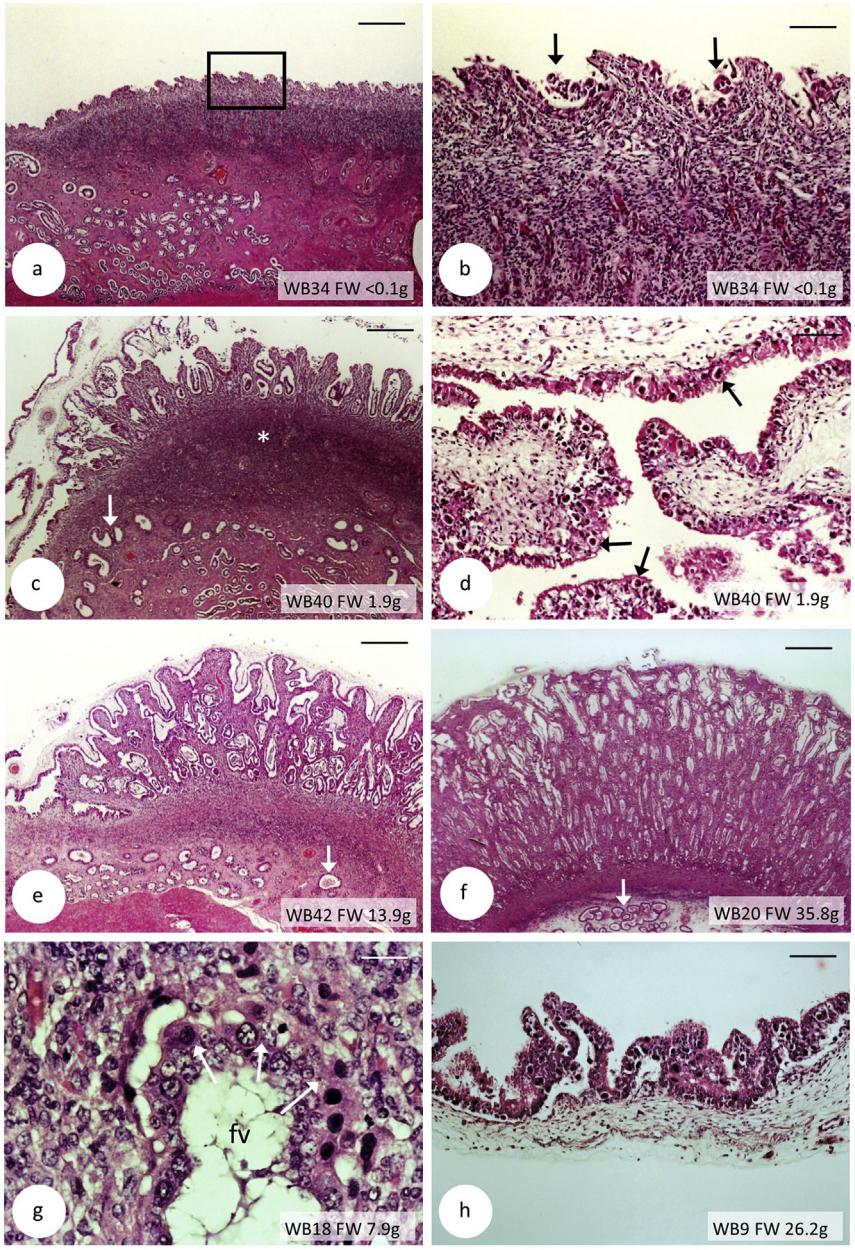

Fig. 3. a) Section of the surface of an endometrial caruncle in WB34 (FW < 0.1 g). Shallow indentations in the lumenal surface herald the beginnings of interdigitation between the allantochorion and endometrium to form a placentome. Note the endometrial glands beneath and to the side of the developing caruncle (scale bar = 500 μm).
b) Higher power section of the boxed area in (a) showing tags of presumed trophoblast cells, many binucleate, left partially attached to the epithelium at the base of the indentations (arrows) Scale bar = 150 μm).
*c) Section of a young placentome in WB40 (FW = 1.9 g) showing the developing interdigitation between villi of allantochorion and pronounced clefts in the stroma of the endometrial caruncle. Post-mortem separation enables clear demarcation between fetal and maternal tissues. Note the density of the stroma (asterisk) and the distended endometrial glands (arrow) at the base of the caruncle (scale bar = 500 μm).
d) Section of the intercotyledonary allantochorion in WB40 (FW = 1.9 g) showing the mix of uninucleate and binucleate (arrowed) trophoblast cells (scale bar = 100 μm).
e) and f) As gestation proceeds the placentomes become increasingly complex but maintain their essentially flat profiles. In the later stage specimen, the chorionic villi within their maternal crypts have become tightly packed together. Endometrial glands persist below the placentome (arrowed; scale bars = 500 μm).
g) High power section in the middle of a placentome in WB18 (FW = 7.9 g) showing the potential for fusion of fetal trophoblast and maternal epithelial cells to form a syncytium (arrows; fv = fetal villus; scale bar = 50 μm)
h) Section of a roughened patch on the intercotyledonary allantochorion of WB9 (FW = 26.2 g) showing the undulations of the trophoblast (scale bar = 100 μm).

placentome (Fig. 6c) and intercotyledonary allantochorion (Fig. 6d). Staining occurred in both the epithelial and stromal cells of the maternal septae, whereas on fetal side staining was limited to the trophoblast cells (Fig. 6e and f). The possibility exists that the staining of the trophoblast and maternal cells could have been caused by diffusion of the reaction product from the BNCs.

3.3. Progestagen production

Table 2 and Fig. 7 show the progestagen concentrations measured in maternal serum and fetal allantoic and amniotic fluids. Serum levels ranged from 1.5 to 5.6 ng/ml between 38 and 67 days. Progestagen concentrations in allantoic fluid (6.5–26.8 ng/ml) were appreciably higher than their maternal serum counterparts, thereby supporting the immunocytochemical staining evidence of progestagen secretion by the placenta, especially its intercotyledonary portion, from an early stage of gestation. A positive relationship existed between the level of progestagens in allantoic fluid and gestational age ($y = 0.5713x - 18.889$; $r = 0.48$; $n = 18$; $P = 0.04$).

Similarly, although concentrations in amniotic fluid were appreciably lower than in allantoic fluid, they did increase significantly as gestation progressed ($y = -0.0084x + 3.5305$; $r = 0.78$; $n = 16$; $P < 0.001$), again indicating the placenta as a potential source of progestagens.

4. Discussion

Of the total of 50 adult, female wildebeest killed in the 5 day culling operation, 43 (86%) were pregnant. Eleven of these pregnant animals (11/43 [26%]) were lactating with a calf at foot, thereby indicating a high level of predation of youngstock by lions, leopards and hyena in this particular population. While these pregnancies were not as tightly grouped as described previously in the massive migratory herds of wildebeest in the Masai Mara [1,4], the fact that they encompassed only the estimated first quarter of the 240 day gestation period nonetheless indicated a well-defined breeding season in this non-migratory population.

The sample provided a unique opportunity to study, grossly and

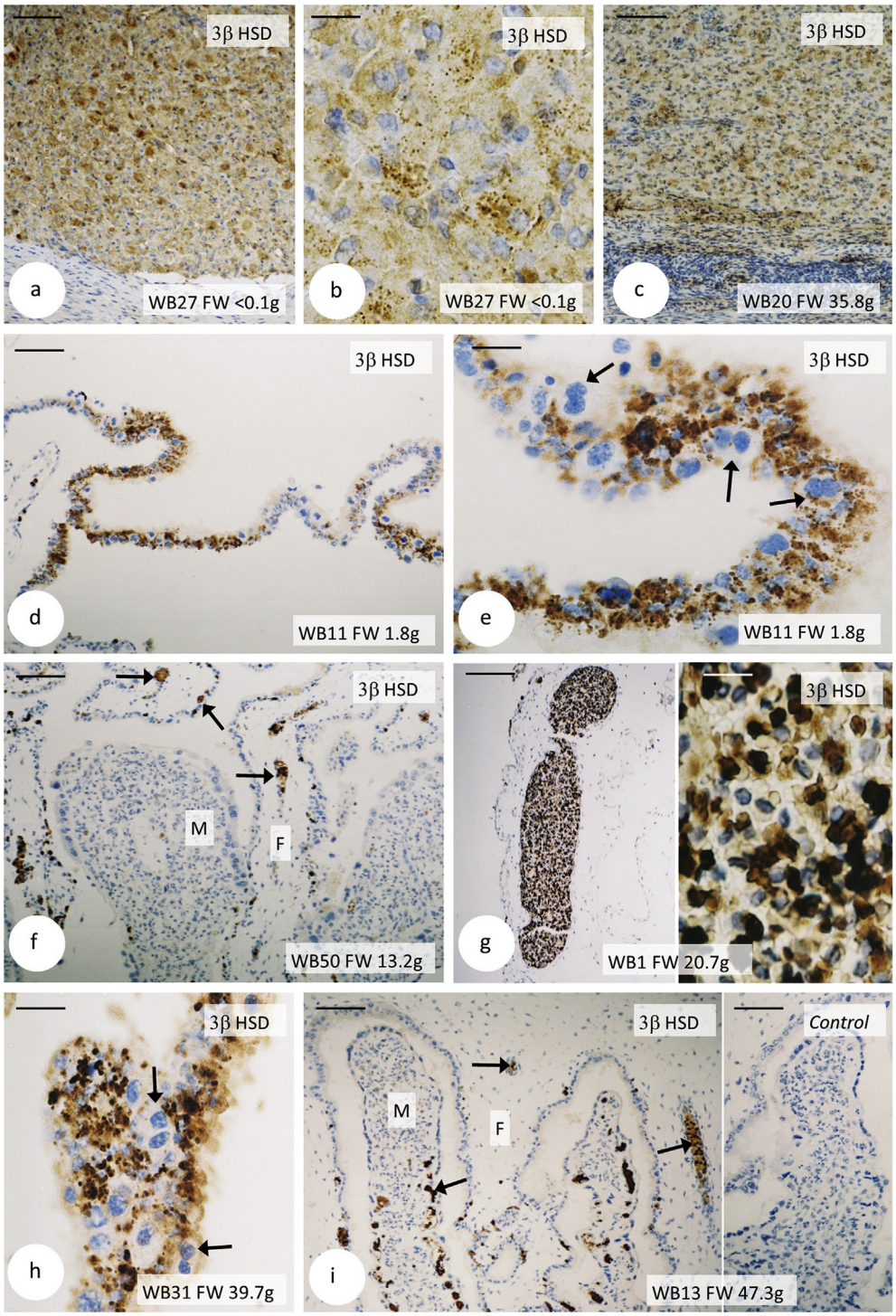

Fig. 4. a - c) Low and higher power sections of the CL in WB27 (FW < 0.1 g) and WB20 (FW = 35.8 g) stained with the 3βHSD antiserum and showing granular staining of some large luteal cells in the young CL. Subjectively, staining appears to be slightly reduced in the older CL of WB20 (scale bars a & c = 150 μm, b = 75 μm).
d & e) Low and higher power sections of the interplacentomal allantochorion in WB11 (FW = 1.8 g) stained with the 3βHSD antiserum. Note the patchy, strong, granular staining (scale bars d = 200 μm, e = 50 μm).
f) Low power section near the fetal surface of a placentome in WB50 (FW = 13.2 g) stained for 3βHSD and showing the lack of staining of fetal trophoblast or maternal epithelial cells within the placentome for this enzyme (scale bar = 200 μm).
g) However, a sub-population of both fetal and maternal erythrocytes stained strongly with the 3βHSD antiserum, which is highlighted at low and higher power in one fetal blood vessel (scale bars = 100 μm, inset = 25 μm).
h & i) The staining pattern with the 3βHSD antibody remained constant in the later stages of gestation examined in both the intercotyledonary allantochorion and the placentome. The negative control shows a complete absence of staining (scale bars, h = 50 μm; i = 200 μm).

histologically, early differentiation and development of the fetal and maternal components of the placenta in this populous plains ungulate, from initial elongation of the allantochorion through to the establishment and functioning of the typical ruminant placentomes that afford maternofetal exchange to maintain fetal growth. Sadly, the inability to perfuse-fix the uteri resulted in some post mortem separation of the fetal and maternal components of the placentome in the early stage specimens. Nevertheless, persisting close attachment of clumps of the typically ruminant BNCs, both at the lumenal surface of the caruncle in the very early stages of gestation and at the maternal base of the placentome soon afterwards, indicated that in the wildebeest, as previously shown and like all wild ruminants examined to date, fusion occurs between BNCs and maternal epithelial cells at the interface of the maternal and fetal tissue [10]. Two patterns of BNC fusion occur. Either they fuse with maternal uterine epithelium cells to form individual tri-nucleate cells (TNCs), or the uterine epithelium is replaced by a continuous persistent fetomaternal syncytial layer formed by repeated BNC migration and fusion after initial TNC formation at implantation. The former is characteristic of cows and all wild ruminants studied to date, while the latter pattern is found in sheep and goats [10]. Interestingly, the wildebeest proves the exception to rule and has a fetomaternal syncytium more akin to the sheep and goat than the cow and other wild ruminants [10]. This fusion of fetal and maternal cells, whatever form it takes, promotes the transfer of fetal derived products

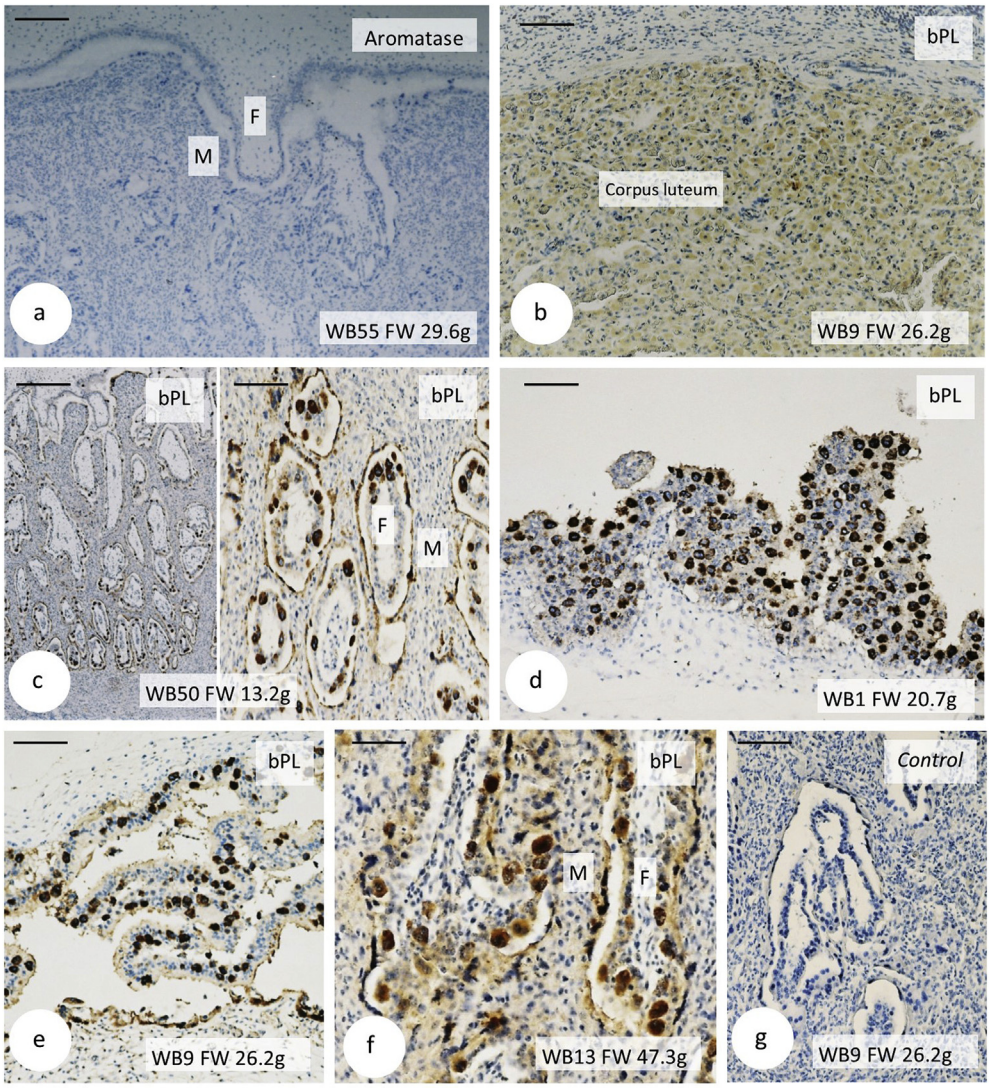

Fig. 5. a) Low power section at the surface of a placentome in WB55 (FW = 29.6 g) negatively stained by the aromatase antibody (F = fetal; M = maternal; scale bar = 200 μm).
b) Low power section of the corpus luteum in WB9 (FW = 26.2 g) showing relatively even staining of both the small and large luteal cells with the bPL antiserum (scale bar = 150 μm).
c) Low and higher power sections of a placentome in WB50 (FW = 13.2 g) stained with the bPL antiserum and showing positive labelling of the BNCs, predominantly at the base of the placentome, and the flattened maternal epithelial cells (scale bars = 200 μm, 100 μm).
d) Section of a patch of the undulating trophoblast growth on the intercotyledonary allantochorion in WB1 (FW = 20.7 g) stained with the bPL antiserum and showing strong positive staining of the BNCs (scale bar = 100 μm).
e) A marginal fold of allantochorion at the lateral edge of the placentome in WB9 (FW = 26.2 g) also showing strong staining of the BNCs (scale bar = 100 μm).
f) High power section at the base of a placentome (WB13; FW = 47.3 g) showing the maternal (M) and fetal (F) villi and the close association of some BNCs with the maternal epithelium (arrowed; scale bar = 75 μm).
g) The negative control shows a complete absence of staining (scale bar = 100 μm).

to support the pregnancy state [14].

Highlighting the BNCs with an antibody specific for bPL showed them to be situated predominantly at the base of the placentome in the wildebeest. However, staining with the PAG-RB antibody, which has been described as the most reliable PAG marker of BNCs in other ruminant species [15], demonstrated an even distribution of BNCs throughout the placentome as noted previously in the wildebeest [10]. As has been shown by other authors [15–17], staining of sub-populations of BNCs within the placentome with different antibodies illustrated that not all BNCs carry out the same function within the placentome. Furthermore, as noted previously [10], we confirmed a continuous linear PAG staining pattern of the fetomaternal syncytium which is more akin to that noted in the sheep and goat than the cow.

The wildebeest showed some aspects of placentation that are noteworthy. First, the copious amounts of endometrial gland secretion produced and accumulated in both the gravid and non-gravid uterine horns, despite the complete physical separation of these two uterine compartments by the bifurcation of the cervix towards its uterine os. In the non-pregnant uteri examined there were no such accumulations of exocrine secretions within the uterine lumen. Hence, the secretions from the endometrial glands in the pregnant animals likely occur in response to pregnancy hormones, such as progesterone, alone or perhaps in combination with placental lactogen, rather than local stimuli from the presence of a conceptus. Whether this inspissated secretion is absorbed later in pregnancy and prior to parturition, or before the post partum female returns to oestrus (mean of 102.4 ± 29.9 days) [4], is not known.

Secondly, another interesting feature of the wildebeest placenta was the development of the irregular patches of trophoblast on the allantochorion between the cotyledons, which, subjectively, appeared to have more BNCs than the other intercotyledonary areas. No corresponding caruncle tissue was evident on the endometrium underlying the patches. Adventitial placentation has been described in cattle where additional sites of cotyledonary villi occur between existing placentomes. This is believed to be a compensatory mechanism as a result of inadequate development of existing placentomes [18], or from a reduction in caruncle numbers due to congenital disorders or inflammation and scarring following repeated episodes of endometritis [19]. Clearly, the intercotyledonary villi in the wildebeest did not stem from a congenital or pathological condition as it was a feature of all the later stage placentae examined. To the authors' knowledge such areas of the placentae of ruminants have not been described before, apart from a report on one placenta of a species of deer (*Cervus mexicanus*) which had cotyledons and diffuse villus areas, with each horn having several dozen tuft-like patches of villi [20]. However, Mossman [6] described this as most likely an anomalous individual. Considering that the earliest ruminant, Tragulus, has a diffuse, non-placentomal placenta it is perhaps worth considering that some other ruminants may have token areas of diffuse placentation remaining. Histological samples of ruminant placentae taken at post mortem frequently focus on the

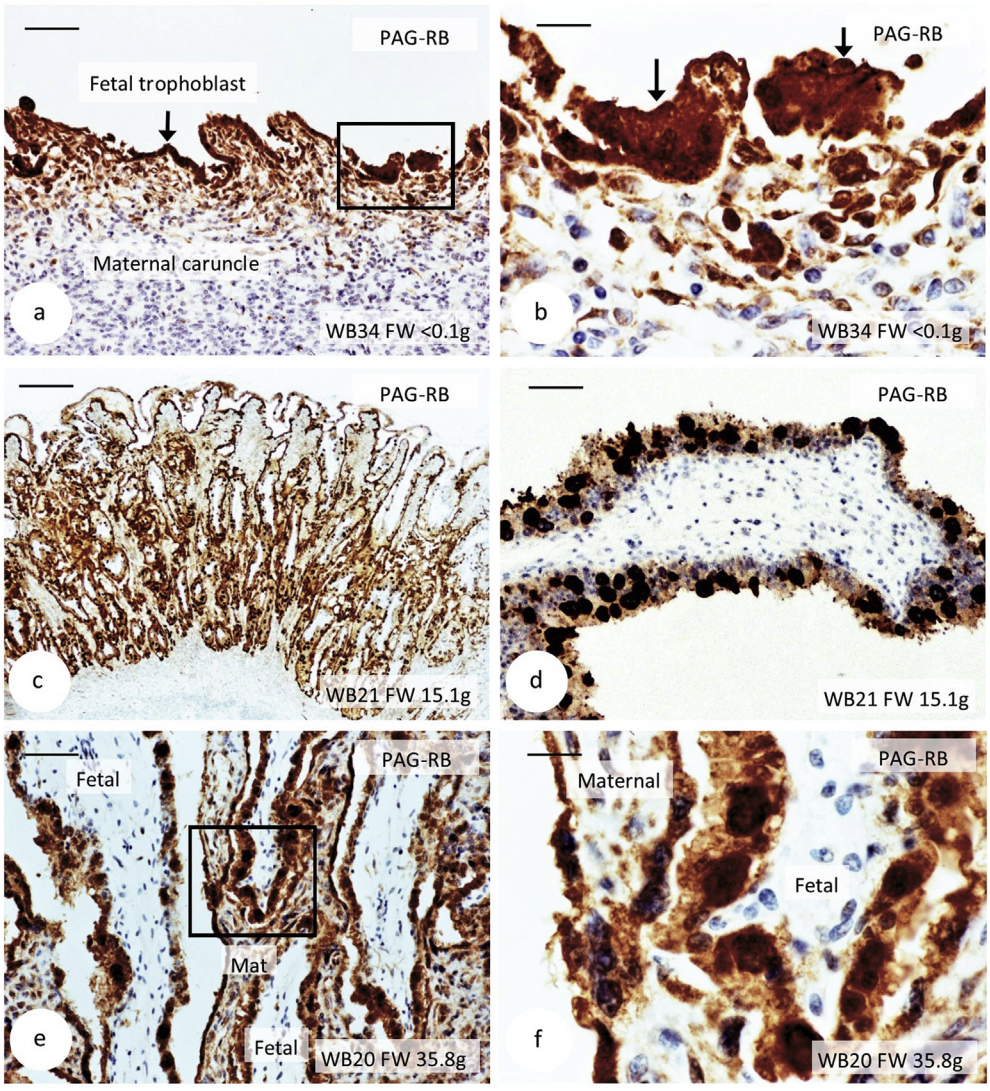

Fig. 6. a) Fetal surface of a very early placentome (WB34; FW < 0.1 g) showing some still adhered trophoblast cells stained positively by the PAG-RB antibody (scale bar = 150 μm).
b) Higher power section of the boxed area in (a) showing some still adhered trophoblast cells stained positively by the PAG-RB antibody (scale bar = 30 μm).
c) Low power section of a placentome from WB21 (FW = 15.1 g) showing strong staining of the BNCs by the PAG-RB antiserum and continuous staining along the edges of the maternal and fetal villi (scale bar = 500 μm).
d) High power section of the intercotyledonary allantochorion (WB21; FW = 15.1 g) showing the dense staining of the BNCs by the PAG-RT antibody. The remaining trophoblast also shows pale staining (scale bar = 50 μm).
Low (e) and high (f) power sections deep within a placentome of WB20 (FW = 35.8 g) stained with PAG-RB antiserum and showing strong staining of the placental syncytium. Note how some stromal cells in the maternal, but not the fetal, villi are also stained (scale bars: e = 75 μm; f = 25 μm).

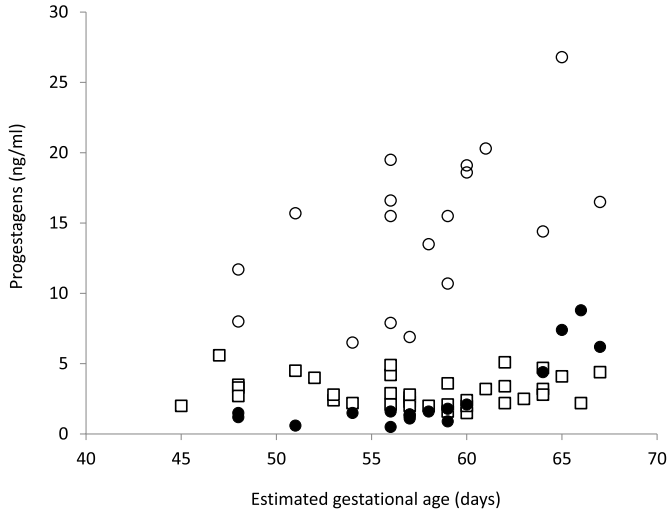

Fig. 7. The relationship between estimated gestational age and progestagens in (a) maternal serum (; y = −0.0084x + 3.5305; r = 0.04; n = 36; P = 0.79); b) allantoic fluid (○; y = 0.5713x - 18.889; r = 0.48; n = 18; P = 0.04); and c) amniotic fluid (●; y = −0.0084x + 3.5305; r = 0.78; n = 16; P < 0.001).

placentomes and more careful examination should probably be made of the intercotyledonary areas as well. Indeed, the placenta of the giraffe shows small regularly spaced tufts of villi in the intercotyledonary areas (S Wilsher and WR Allen, unpublished observations).

As shown previously [1], the single ovulatory CL of pregnancy remains present in the ipsilateral maternal ovary throughout gestation in the wildebeest, but regresses during mid gestation by about 16%, before gaining size towards the end of pregnancy. Measurement of fecal progestagen concentrations in pregnant wildebeest showed an initial rise after copulation and continuation of the elevated levels until parturition; fluctuations in progestagen concentrations between individuals throughout pregnancy resulted in no distinct longitudinal excretion profile [4]. In the present study the CL retained the ability to synthesise progesterone throughout the period studied as demonstrated by the immunolocalization of 3βHSD in the luteal cells. In addition, using the 3BHSD antibody as described, the intercotyledonary, but not the cotyledonary, areas of the placenta also exhibited the ability to synthesise progesterone from very early in gestation. Since only early gestation tissue was available, 3 βHSD activity in the later stages of pregnancy in the wildebeest remains to be determined. Certainly, in cattle cotyledons 3βHSD activity has been demonstrated from at least 4 months of gestation, and is markedly enhanced during the third trimester [21].

This, together with the finding of increasing concentrations of progestagens in allantoic and amniotic fluids, suggests that the wildebeest placenta may potentially contribute to progestagen levels locally

early in pregnancy. Using the progesterone ELISA assay described, no increase in serum progestagen concentrations was observed during early gestation despite the steadily increasing area of intercotyledonary placenta during the period studied. In domestic ruminants, both the CL and the placenta play roles in supporting pregnancy via progesterone secretion. In the sheep the maintenance of pregnancy after day 50 of gestation depends on secretion of progesterone by the placenta; ovariectomy before day 50 results in abortion whereas pregnancy continues in the majority of animals from which the ovaries are removed after this time [22,23]. In the cow, on the other hand, the CL is essential to maintain pregnancy prior to days 165–180 although support from the CL is desirable during later pregnancy to prevent a shortening of gestation and abnormal parturition [24].

A further twist to potential sources of progestagens during pregnancy in the wildebeest is the strong staining of a sub-population of erythrocytes in both the maternal and fetal blood vessels within the placentome by the 3βHSD antiserum. Previous studies have shown the presence of steroid dehydrogenases in human erythrocytes [25] and their permeability to the steroid sex hormones [26]. Furthermore, whole blood from pregnant Rock Hyrax (*Procavia capensis*) has the ability to metabolise progesterone to 5α-pregnanes [27,28] and fetal erythrocytes in sheep and cows can convert progesterone to 20α-hydroxyprogesterone [29]. More specifically, the steroid enzyme in question, 3βHSD, has been localized to rat erythrocytes [30]. In the present study on the wildebeest it was not possible to confirm the immunostaining results by measuring 3βHSD enzyme activity in cultures or undertaking western blots and more stringent investigation is required to confirm these findings. Furthermore, apart from converting pregnenolone to progesterone, 3βHSD can also stimulate the conversion of 17α-hydroxypregnenlone to 17α-hydroxyprogesterone, dehydroepiandrosterone (DHEA) to androstenedione, androstenediol to testosterone and androstadienol to androstadienone, thereby showing its numerous functions dependent on its location in the body and the type of isoenzyme it is expressed as [31]. Added to this, there are a number of species-specific 3βHSD enzymes [31]. So if, indeed, the steroid enzyme 3βHSD is present in wildebeest maternal and fetal erythrocytes its role in steroid metabolism may be something other than converting pregnenolone to progesterone.

Using the cytochrome P450 aromatase antibody at the concentration stated no component of the placenta stained positively for aromatase at any stage of gestation studied. In cattle aromatase activity has been detected in bovine cotyledons from at least 4 months of gestation with peaks at 5 months and term [32]. Likewise, in goats P450-aromatase mRNA was found to be expressed in placental microvilli from early in gestation, with expression and distribution of the enzyme increasing throughout pregnancy [33]. Since the present study only examined early stage pregnancies using immunohistochemistry, further sampling, particularly of later stage wildebeest placenta, would be a useful to determine if P450-aromatase activity can be detected immunohistochemically or by other means.

In line with other ruminant placentae the BNCs [14], especially those in the intercoyledonary allantochorion, stained strongly with the bPL antiserum indicating their production of this lactogenic hormone during early gestation. Ruminant PL may also be involved in prolonging the lifespan and stimulating the secretory function of the maternal CL throughout gestation, promoting mammary growth and/or partitioning of nutrients between the mother and fetus [34].

In summary, the wildebeest generates a typical macrocotyledonary placenta in one uterine horn which is synepitheliochorial in its intimate association with the endometrium and which, most likely as in sheep, establishes a syncytial fusion between BNCs and maternal epithelial cells to facilitate physical transfer of lactogenic and glycoprotein hormones from the placenta to the mother. Placental lactogen, pregnancy associated glycoprotein and the enzyme 3βHSD that converts pregnenolone to progesterone were all immunolocalized to the placenta of the wildebeest.

Conflicts of interest

None.

Declarations of interest

None.

Funding

The research did not receive any specific grant from funding agencies in the public, commercial or not-for-profit sectors.

Acknowledgements

The authors are sincerely grateful to the Manager, Mr Blondie Latham, and his staff at the Bubye Hunting Conservancy, Zimbabwe, for their generous hospitality and for much practical assistance. They also thank Mrs Susan Gower and the Animal Health Trust, Newmarket for histological and immunocytochemical expertise and help.

References

[1] R.M. Watson, Reproduction of Wildebeest, *Connochaetes taurinus*, in the Serengeti region and its significance to conservation, J. Reprod. Fertil. Suppl 6 (1969) 287–310.
[2] R.D. Estes, R.K. Estes, The birth and survival of Wildebeest calves, Z. Tierpsychol. 50 (1979) 45–95.
[3] L.M. Talbot, M.H. Talbot, The Wildebeest in Western Swaziland, East Africa. Wildlife Monographs No. 12, The New York Zoological Society, New York, 1963.
[4] A.M. Clay, R.D. Estes, K.V. Thompson, D.E. Wildt, S.L. Honfort, Endocrine patterns of the oestrous cycle and pregnancy of Wildebeest in the Serengeti ecosystem, Gen. Comp. Endocrinol. 56 (2010) 365–371 https://doi: 10.1016/j.ygcen.2009.12.005.
[5] P. Hradrecký, Uterine morphology in some African antelopes, J. Zoo Anim. Med. 13 (1982) 132–136.
[6] H.W. Mossman, Comparative anatomy of the oviduct, uterus and vagina, in: H.W. Mossman (Ed.), Vertebrate Fetal Membranes, Macmillan Press, Basingstoke, Hants, UK, 1987, pp. 63–74.
[7] P. Hradecký, Placental morphology in African antelopes and giraffes, Theriogenology 20 (1983) 725–734.
[8] P. Hradecký, H.W. Mossman, G.G. Scott, Comparative histology of antelope placentomes, Theriogenology 29 (1988) 693–714.
[9] K. Benirschke, Comparative placentation, http://placentation.ucsd.edu/gnu.html, (2007) , Accessed date: 3 January 2019.
[10] F.B. P Wooding, D. Osborn, G.J. Killian, Trinucleate uterine epithelial cells as evidence for White-tail Deer trophoblast binucleate cell migration and as markers of placental binucleate cell dynamics in a variety of wild ruminants, Placenta 62 (2018) 34–42, https://doi.org/10.1016/j.placenta.2017.12.012.
[11] A.S. Huggett, W.F. Widdas, The relationship between mammalian fetal weights and conception age, J. Physiol. 114 (1951) 306–317.
[12] S. Wilsher, F. Stansfield, R.E. Greenwood, P.D. Trethowan, R.A. Anderson, F.B. Wooding, W.R. Allen, Ovarian and placental morphology and endocrine functions in the pregnant giraffe (*Giraffa camelopardalis*), Reproduction 145 (2013) 541–554, https://doi.org/10.1530/REP-13-0060.
[13] W.R. Allen, M.W. Sanderson, The value of a rapid progesterone assay (AELIA) in equine stud veterinary medicine and management, Proceedings of the 9th Bain-Fallon Memorial Lectures, AEVA, Sydney, 1987, pp. 75–82.
[14] F.B. Wooding, G. Burton, Synepitheliochorial placentation: ruminants (Ewe and cow), in: F.B. Wooding, G. Burton (Eds.), Comparative Placentation, Springer-Verlag Heidelburg, Berlin, 2008, pp. 133–167.
[15] F.B. Wooding, S. Wilsher, K. Benirschke, C.J. Jones, W.R. Allen, Immunocytochemistry of the placentas of giraffe (*Giraffa cameleopardalis giraffa*) and okapi (*Okapi johnstoni*): comparison with other ruminants, Placenta 36 (2015) (2015) 77–87, https://doi.org/10.1016/j.placenta.2014.10.010.
[16] J.A. Green, S. Xie, X. Quan, B. Bao, X. Gan, N. Mathialagan, J.-F. Beckers J-F, R.M. Roberts, Pregnancy associated bovine and ovine glycoproteins exhibit spatially and temporally distinct expression patterns during pregnancy, Biol. Reprod. 62 (2000) 1624–1631.
[17] E. Touzard, P. Reinaud, O. Dubois, C. Guyader-Joly, P. Humblot, C. Ponsart, G. Charpigny, Specific expression patterns and cell distribution of ancient and modern PAG in bovine placenta during pregnancy, Reproduction 146 (2013) 347–362, https://doi.org/10.1530/REP-13-0143.
[18] T.C. Jones, R.D. Hunt, N.W. King, Veterinary Pathology, sixth ed., Williams & Wilkins, Baltimore, Maryland, 1997, pp. 1178–1179.
[19] P.C. Kennedy, R.B. Miller, The female genital system, in: K.V. F Jubb, P.C. Kennedy, N. Palmer (Eds.), Pathology of Domestic Animals, fourth ed., vol 3, Academic Press, Inc., San Diego, California, 1993, pp. 390–391.
[20] W. Turner, On the cotyledonary and diffused placenta of the Mexican deer (*Cervus mexicannus*), J. Anat. Physiol. 13 (1879) 195–200.

[21] S. Tsumagari, J. Kamata, K. Takagi, K. Tanemura, A. Yosai, M. Takeishi, 3 beta-Hydroxysteroid dehydrogenase activity and gestagen concentrations in bovine cotyledons and caruncles during gestation and parturition, J. Reprod. Fertil. 102 (1994) 35–39.
[22] L.E. Casida, E.J. Warwick, The necessity of the corpus luteum for maintenance of pregnancy in the ewe, J. Anim. Sci. 4 (1945) 34–36.
[23] R. Denamur, J. Martinet, Effects de l'ovariectomie chez la brebis pendant la gestation, Comptes Rendus Seances Soc. Biol. Ses Fil. 149 (1955) 2105–2107.
[24] V.L. Estergreen Jr., O.L. Frost, W.R. Gomes, R.E. Erb, J.F. Bullard, Effect of ovariectomy on pregnancy maintenance and parturition in dairy cows, J. Dairy Sci. 50 (1967) 1293–1295.
[25] E. Mulder, G.J.M. Lamers-Stahhofen, H. J Van der Molen, Isolation and characterization of 17β-hydroxy steroid dehydrogenase from human erythrocytes, Biochem. J. 127 (1972) 649–659.
[26] P. Koefoed, J. Brahm, The permeability of human red blood cell membrane to steroid sex hormones, Biochim. Biophys. Acta 1195 (1994) 55–62.
[27] R.B. Heap, S. Gombe, J.B. Sale, Pregnancy in the hyrax and erythrocyte metabolism of progesterone, Nature 257 (1975) 809–811.
[28] S. Kirkman, E.D. Wallace, R.J. van Aarde, H. C Potgieter, Steroidogenic correlates of pregnancy in the rock hyrax (*Procavia capensis*), Life Sci. 68 (2001) 2061–2072.
[29] C.D. Nancarrow, Decline with age in the rate of production of progesterone to 20a-hydroxypregn-4-en-3-one in the blood of perinatal ruminants, Aust. J. Biol. Sci. 36 (1983) 183–190.
[30] W. Heyns, P. De Moor, A 3(17)beta-hydroxysteroid dehydrogenase in rat erythrocytes. Conversion of 5alpha-dihydrotestosterone into 5alpha-androstane-3beta,17beta-diol and purification of the enzyme by affinity chromatography, Biochim. Biophys. Acta 358 (1974) 1–13.
[31] J. Simard, M.L. Ricketts, S. Gingras, P. Soucy, F.A. Feltus, M.H. Melner, Molecular biology of the 3β-hydroxysteroid dehydrogenase/Δ5.-Δ4 isomerase gene family, Endocr. Rev. 26 (2005) 525–582.
[32] S. Tsumagari, J. Kamata, K. Takagi, K. Tanemura, A. Yosai, M. Takeishi, Aromatase activity and oestrogen concentrations in bovine cotyledons and caruncles during pregnancy and parturition, J. Reprod. Fertil. 98 (1993) 631–636.
[33] J.A. Mondragon, R. Ocadiz-Delgado, C. Miranda, J. Valencia, A.M. Rosales, P. Gariglio, M.C. Romano, Expression of P450-aromatase in the goat placenta throughout pregnancy, Theriogenology 68 (2007) 646–653.
[34] J.C. Byatt, W.C. Warren, P.J. Eppard, N.R. Staten, G.G. Krivi, R.J. Collier, Ruminant placental lactogens: structure and biology, J. Anim. Sci. 70 (1992) 2911–2923.